

ELECTRON OPTIC DESIGN OF ARRAYED E-BEAM MICROCOLUMNS BASED SYSTEMS FOR WAFER DEFECTS INSPECTION

V.V. Kazmiruk, T.N. Savitskaja

*Institute of Microelectronics Technology and High Purity Materials, Russian Academy
of Sciences*

Abstract

In this paper is considered a matter of the system for wafer defect inspection (WDIS) practical realization. Such systems are on the agenda as the next generation and substitution for light optics and single e -beam based WDISs.

Introduction

At the present time an activity in the field of e -beam microcolumns practical realization is growing up rapidly. The most significant progress is attained by groups of T.H.P. Chang from IBM Research Center [1], P. Kruit from Delft Technical University [2–6] and H.S. Kim and alii [7, 8].

However, their efforts directed mainly on e -beam lithography application or just microcolumn electron optics design.

In this paper is considered a matter of the system for wafer defect inspection (WDIS) practical realization. Such systems are on the agenda as the next generation and substitution for light optics and single e -beam based WDISs.

In our previous work [9] the requirements to WDIS have been considered as informative system with resolution down to 2 nm. It was shown that in the range of 10–30 nm multibeam WDIS for topographical defects inspection would be comparable in throughput with the light optics system when number of columns in the array is about 1000. In the case of the line width measuring (LWM) or surface microrelief reconstruction can be realized resolution 2–10 nm.

Are considered aspects of WDIS design for both application.

The electron optics design

First of all consider the main principles of electron optics design of the microcolumn. We start from simple single lens column used by many authors [1, 8] for experiments in this field.

The electron optical components of a one lens column are shown schematically in fig. 1.

The resolution of the microscope column is limited primarily by the aberrations of the objective lens. The probe size is given by:

$$d_b^2 = (M \cdot d_0)^2 + d_d^2 + d_s^2 + d_c^2, \quad (1)$$

where M is the column magnification; d_0 is the virtual source size;

$$d_d = 1,5 \cdot \alpha V^{(0,5)} \quad (2)$$

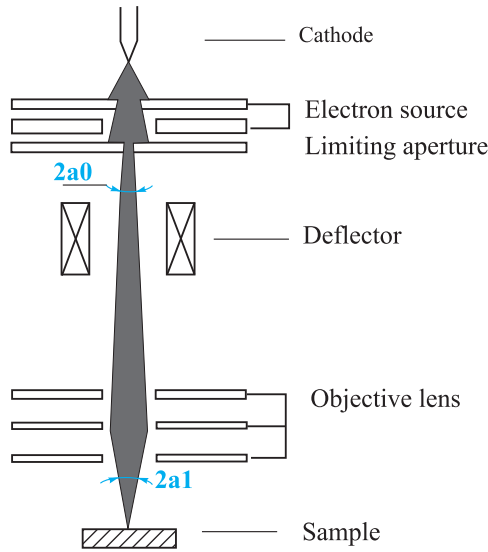


Fig. 1. A one lens column for e -beam lithography

is the diameter of the diffraction disk so that $d_d/2$ is full width half maximum of corresponding distribution.

$$d_s = 1/2 \cdot C_s \alpha^3$$

is the spherical aberration disc with the spherical aberration coefficient C_s ;

$$d_c = C_c \alpha \Delta V / V$$

is the chromatic aberration disk with C_c being aberration coefficient and DV being the energy spread of the beam;

$$\alpha_0 = \alpha \cdot M, \quad (3)$$

where α_0 is the semi convergent angle at the exit of the source and α is the semi convergent angle at the target. Final probe current I_b is

$$I_b = p \alpha_0^2 dI_0 / d\Omega_0. \quad (4)$$

Here $dI_0/d\Omega_0$ is angular emission density.

We use the conventional rule (1) to estimate the chromatic and spherical aberration coefficients of the objective lens: C_c and C_s .

Fig. 2 shows the performance of 1 keV microcolumns with two different objective lenses [1]. The first in solid line, represents a *fixed* symmetric einzel lens. This lens has a 200 μm bore diameter and 250 μm spacing. The lens, operating for a 1 mm working distance in the accelerating mode, has a chromatic and spherical aberration coefficients of approximately 2 mm and 50 mm respectively. As shown in the figure, a probe size of 9,9 nm can be achieved at an optimum semiconvergent angle of $\approx 6,3$ mrad. Further improvement of resolution can be achieved by optimizing the electrodes geometry for working distance 1 mm, that allows to decrease both spherical and chromatical coefficients to values shown by dashed lines. As a result the resolution 8,8 nm

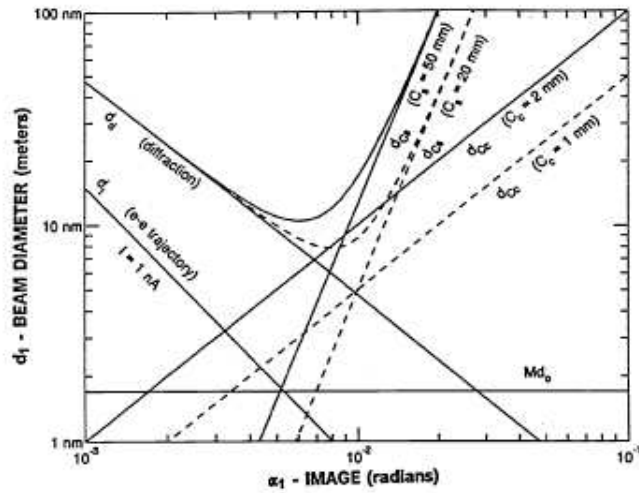


Fig. 2.

at working distance 1 mm can be achieved. These are typical results achieved practically so far [1, 8].

It should be noted that those results achieved in transmission mode, and working distance 1 mm is chosen to place on-axis detector between lens and sample as it shown in fig. 3.

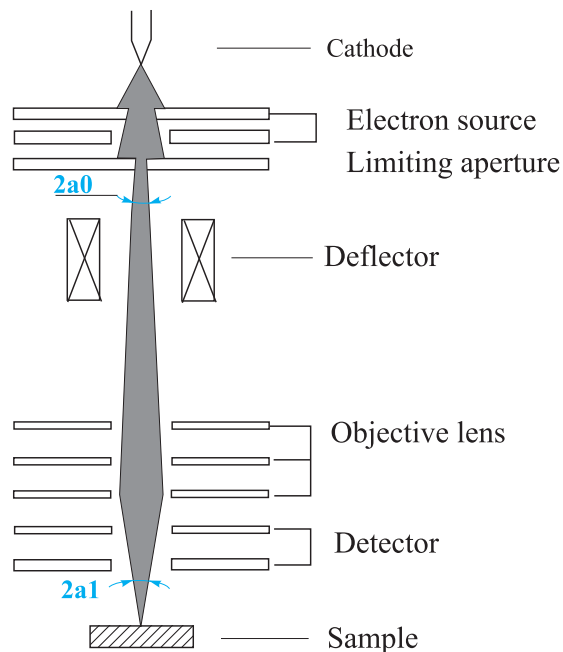


Fig. 3. A one lens microcolumn with on-axis detector

Now consider what should be changed for improving a resolution to 2 nm. Is assumed that electrons energy still is 1 keV and the energy spread $\Delta V = 1$ eV. In the fig. 4 is shown an electron optical performance of 1 keV improved column for $C_s = 0,3$ mm, $C_c = 0,084$ mm.

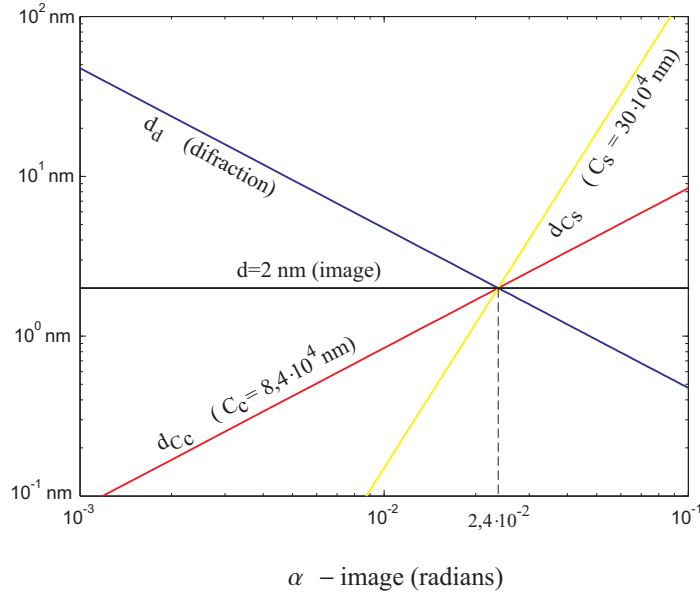


Fig. 4. Electron optical performance of 1 keV improved column.
 $C_s = 0,3$ mm, $C_c = 0,084$ mm

It is obvious from (1) that the value $d_b = 2$ nm can be achieved when each of d_d , d_s , d_c , is less than that value. Thus, diffraction limit becomes a dominating factor which determines semi convergent angle. If is chosen $\alpha \gg 2,4 \cdot 10^{-2}$ radians, then aberration coefficients $C_s \ll 0,3$ mm and $C_c \ll 0,08$ mm. For more exact evaluation examine the residual

$$d^2 - (d_d^2 + d_c^2 + d_s^2) = (M d_0)^2$$

at $d_b = 2$ nm and minimize $(d_d^2 + d_c^2 + d_s^2)$ over α .

Thus for given aberration coefficients C_s and C_c the maximum value of $(M d_0)^2$ can be calculated.

Figures 5, 6 show result for $C_c = 0,04$ and $C_c = 0,02$ mm.

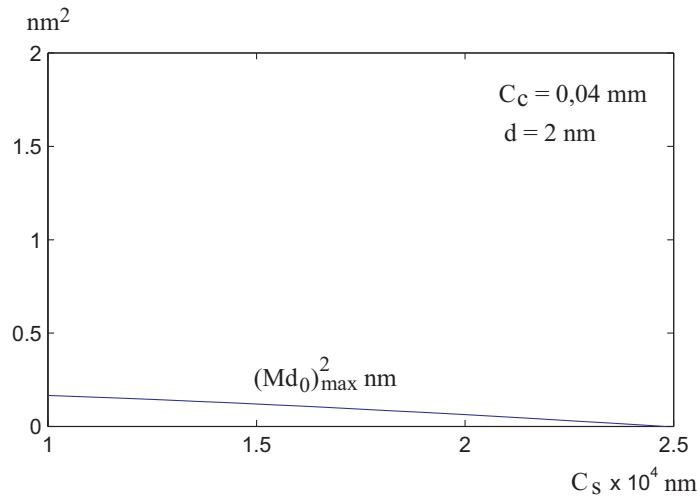


Fig. 5.

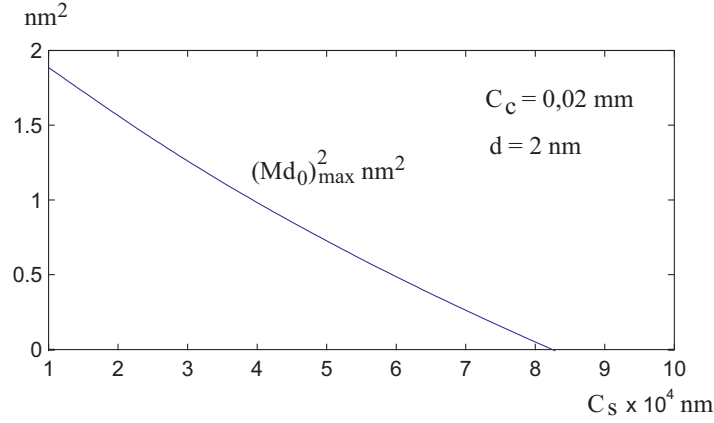


Fig. 6.

Thus, to receive the probe size 2 nm for objective lens with the chromatic aberration coefficient $C_c = 0,04$, the spherical aberration coefficient C_s needs to be lower 0,02 mm and semiconvergent angle $\alpha > 2,6 \cdot 10^{-2}$ rad.

Similarly for $C_c = 0,02$ mm $C_s \leq 0,08$ mm and $\alpha > 2,7 \cdot 10^{-2}$ rad is required.

The use another formulas for probe size diameter calculation, for example [2], gives no principal change to order of C_s and C_c values.

Such a way from the above analytical performance consideration follows that for improvement of the resolution to 2 nm it's necessary to keep semi convergent angle more than $2,7 \cdot 10^{-2}$ rad and radically decrease both chromatical and spherical aberrations coefficients.

Methods of improvement aberrations consist in electrostatic lens dimensional scaling down from conventional lens. In fig. 7 is schematically shown spherical aberration for a positive and a negative lens, illustrated with two rays entering the lens at different radii, r_1 and r_2 . In both cases, the intercept with the z -axis shifts in the negative z direction for increasing radius of incidence.

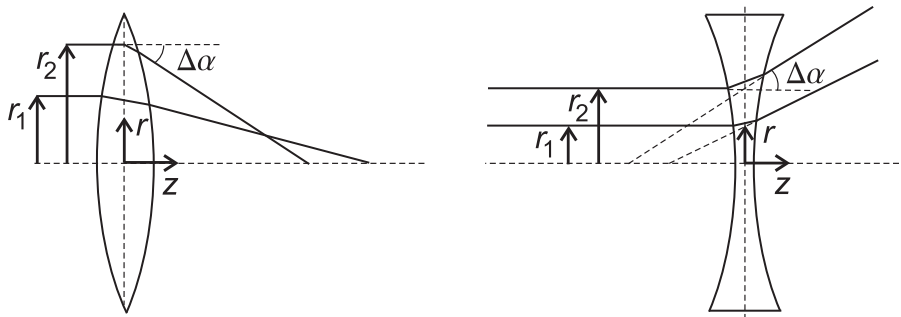


Fig. 7. Spherical aberration for positive and negative lens

By decreasing lens bore diameter and, therefore, radius of incidence r to a few microns is possible to achieve even less values than $C_c = 0,02$ mm $C_s \leq 0,08$ mm. Unfortunately, we should keep the value of semi convergent angle $\alpha \geq 2,7 \cdot 10^{-2}$ rad, which leads the working distance shortening.

As working distance $WD = r/\alpha$, then for incidence radius in the range $2 \div 10 \mu\text{m}$ WD should be in the range $74 \div 370 \mu\text{m}$. Such short working distance does not give enough space for detector placement.

In practice α is even more than $2,7 \cdot 10^{-2}$ rad in order to obtain small diffraction term.

Table 1. Two lens system performance

Probe size	1,73 nm
Probe current	1 nA
Magnification (specimen – gun)	–2,31
C_s gun side	0,68 mm
C_c gun side	0,037 mm
Spherical aberration term	0,92 nm
Chromatic aberration term	0,53 nm
Diffraction term	1,04 nm

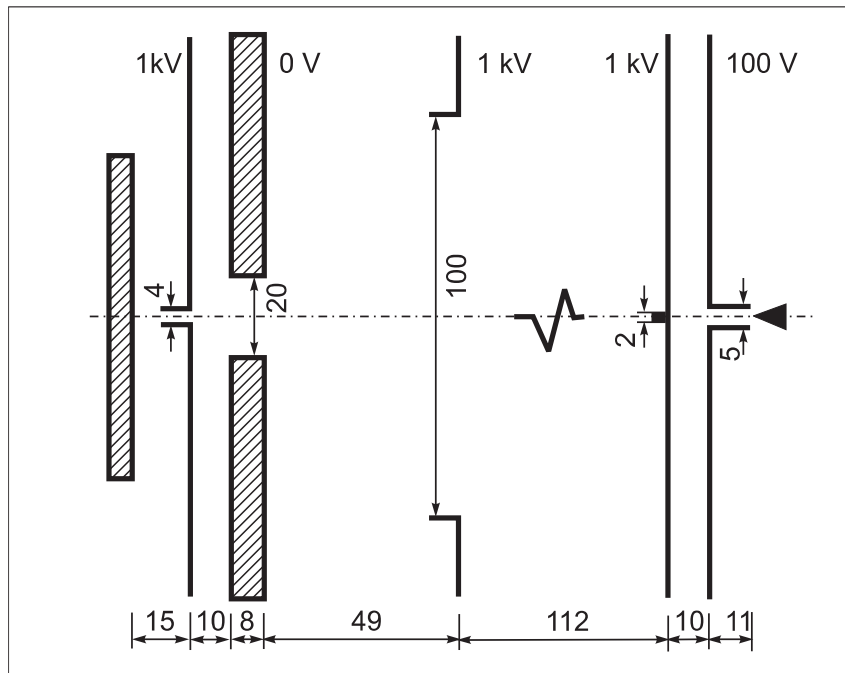


Fig. 8. Optimized two lens system for $WD = 15 \mu\text{m}$ [10]

As an example in fig. 8 is shown an optimized five electrode (two lens) system for $WD = 15 \mu\text{m}$ ($\alpha = 0,13$ rad) and object to image distance $215 \mu\text{m}$. In tab. 1 is depicted the system performance.

The short WD brings a lot others inconveniences besides mentioned above problems with detector placement. First of all these are vacuum deterioration between sample and the system, risk of wafer damaging and small depth of focus. That's why the ideas about an application of such systems are directed mainly on lithography or average resolution low voltage SEM.

Ultra thin film foil implementation for improvement the miniature beam system performance

There are two promising applications of ultra thin foils for electron microscopy: the tunnel junction emitter and the low energy corrector. Common for both applications is that the electron beam is sent through the thin foil at low energy. Measurements of mean free path for number of metals indicate the value about 5 nm at the energy ≈ 5 eV above the Fermi level.

First achieved by us [6] free standing foils have been 5 nm of thickness and later we achieved foils with thickness 4, 3 and even 2,2 nm. A substantial part of electrons can be transmitted through such thin film without scattering, so film acts as an ideal energy filter.

The tunnel junction emitter

Electron field emitters are used in a wide variety of applications, such as: electron microscopes, electron beam lithography machines, field emission displays and vacuum micro electronics. Field emitters have some important advantages over thermionic emitters: they have a higher brightness and lower energy spread, they can operate at ambient temperature and they have a lower power consumption because no heating of a filament is required.

Nevertheless, improvements are still desirable. For example, as it is shown above, the spatial resolution in low voltage electron probes is limited in part by the energy spread of the field emitter. If it would be possible to operate a field emitter at low voltage, battery driven applications are in reach (e. g. displays for laptop computers). The tunnel junction emitter is expected to combine the properties of low energy spread, high brightness, operation at low voltage and low power consumption.

The tunnel junction emitter [2] is constructed by placing a sharp tip within tunneling range of a very thin metal foil (see fig. 9). Between tip and foil a voltage larger than the work function of the foil surface is applied. Provided that the foil is sufficiently thin, a fraction of the tunneled electrons will travel through the foil without scattering. Electrons with sufficient forward energy to overcome the work function are emitted into the vacuum. In this way the work function acts as a high-pass energy filter. Combined with the fact that the electrons originate from an atomic size tunneling area, a monochromatic high-brightness electron source is expected. As for most metals the work function is of the order of a few eV, the source is operated at low voltage. Although the emitted current is only a fraction of the tunnel current, the power consumption is still low because of the low voltage operation and because no heating is required. The emitter can be operated at high frequency because only a small voltage difference is needed to switch between on and off and because the size of the emitter, and therefore its capacitance, can be kept small. This could be interesting for RF applications.

As a tip is assumed to implement very sharp tungsten tip (often called nanotip) similar to that for STM investigations [11]. However, the experiments with clean nanotip and free standing foil as it sketched in fig. 9 have shown

that thin film is damaging in a short time. That happens because of attractive forces between tip and foil.

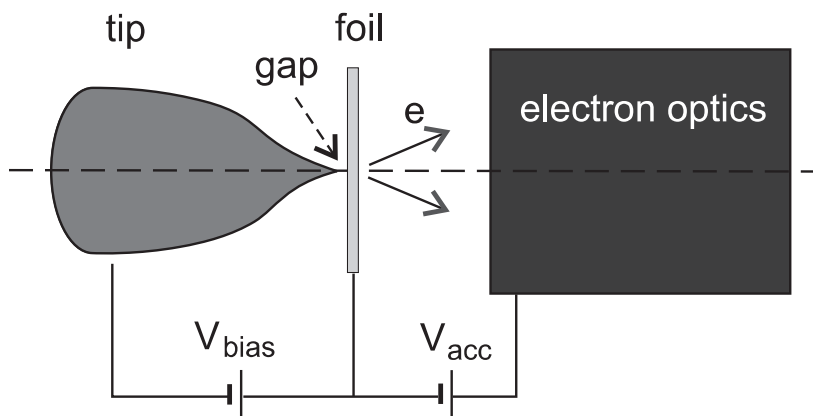


Fig. 9

To avoid this problem was proposed another [3] configuration of experiments (see fig. 10).

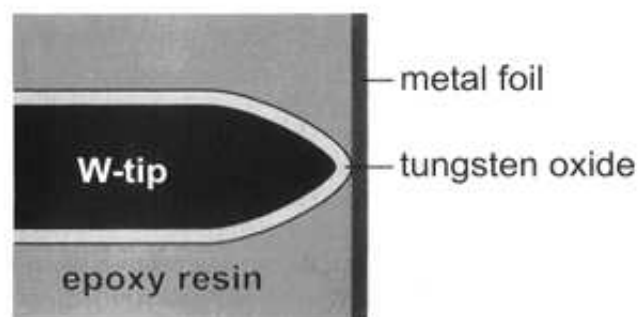


Fig. 10. Cross section sketch of the device [3]

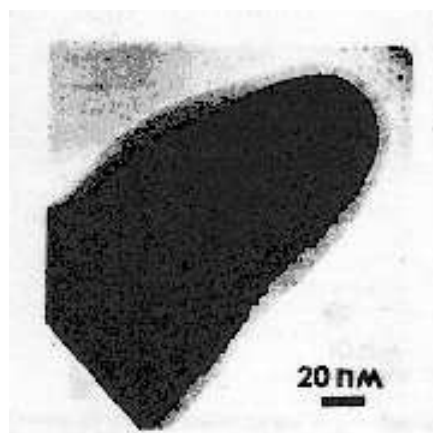


Fig. 11. TEM micrograph of 9V dc etched oxide covered tungsten tip [11]

As a tip was used an oxidized tungsten tip shown at fig. 11.

The experimental work has verified the principle of operating of this emitter. However, the stability and life time are not sufficient enough and still have to be improved. Nevertheless there is a hope that after some optimization of oxide layer, choice of proper tip material and development of reliable assembling technology would be possible to create a working device.

It should be noted one more attractive property of solid state emitter that it is expected to be not that critical to vacuum condition as convenient field emitter.

The low energy aberration corrector

In the basic form corrector is sketched in fig. 12.

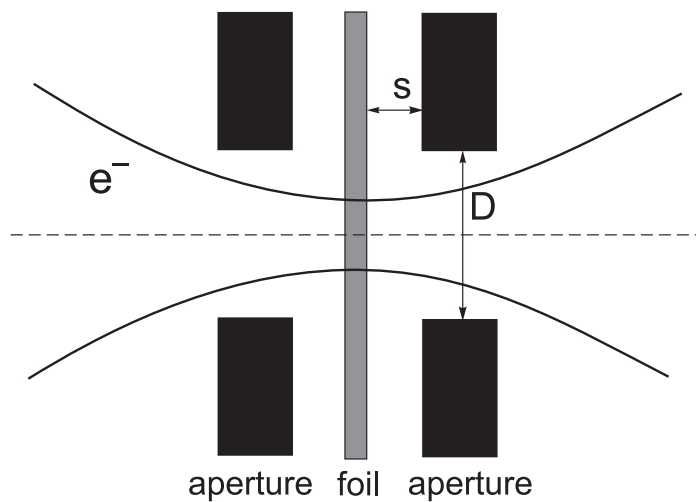


Fig. 12. Basic design of the foil corrector (not to scale). D: diameter of the aperture; s: gap between foil and aperture [4]

It consists of a flat free-standing foil of nanometer size thickness with apertures on both sides. In the low-energy foil corrector, the foil is put on a retarding potential, such that the electrons have almost 0 eV kinetic energy when they enter the foil (and also when they have just left the foil at the other side).

For use in a SEM additional optics is necessary to adjust correction and to focus the beam. A SEM column with corrector is shown at fig. 13.

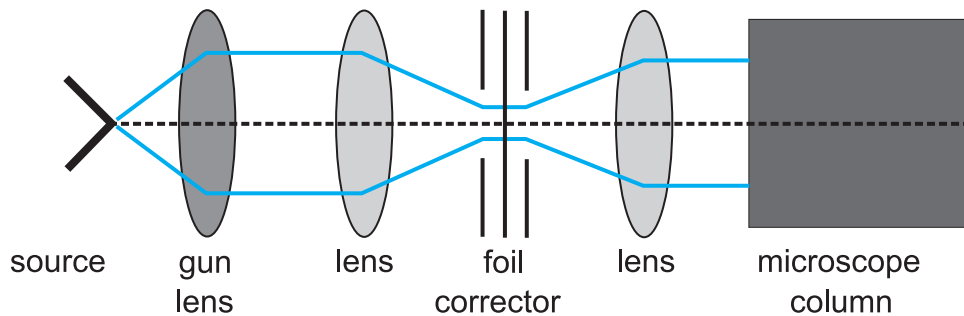


Fig. 13. SEM column with the foil corrector

As corrector is very strong negative lens it is necessary to put focussing lenses close to it. Because of that reason are favorable electrostatic lenses.

Leaving apart all details of corrector calculations (see for details [12]) we present a final result — a calculation example on realistic set-up, e. g. aberration corrected low voltage SEM (see fig. 14).

In the tab. 2 the measures of the design are given and electrode potentials and calculation result for optimum setting are given in the tab. 3.

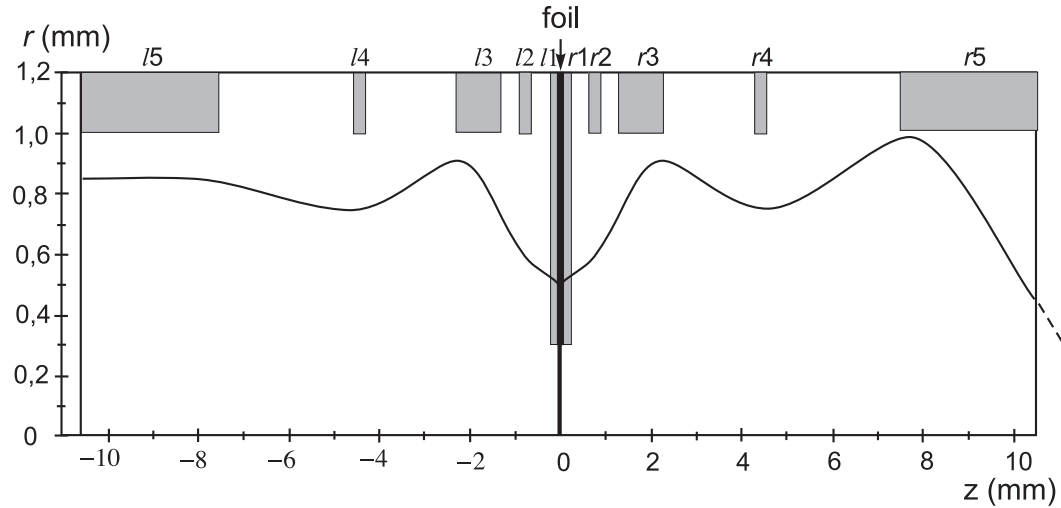


Fig. 14. Design of a low-voltage SEM column with a low-voltage foil corrector [5]. The design is rotationally symmetric in the z -axis

Above the drawing, the numbering of the electrodes is designated. In the drawing, the paraxial ray for the settings in tab. 3 is shown. For the visibility, its radial extent is drawn 5 times larger than the maximum beam radius. Note that this ray has started in fin object position which is far left from the left border, thus it enters the column with a very small, but non-zero slope.

Table 2. Measures of the column design in fig. 14. The design is mirror symmetric in the foil, only the measures for the electrodes at the right side are listed

electrode no.	thickness (mm)	aperture radius (mm)	distance to next electrode (mm)
foil	0	—	0,04
$r1$	0,20	0,30	0,40
$r2$	0,25	1,00	0,40
$r3$	1,00	1,00	2,00
$r4$	0,25	1,00	3,00
$r5$	3,00	1,00	—

Table 3. Optical properties calculated with aberration integrals for a foil potential of respectively 0,1, 0,4 and 1,0 V. The potentials of the other electrodes with respect to the foil are the same as in tab. 2

optical property	aberration integrals	ray tracing	electrode no.	potential (V)
Z_0	-394 mm	-515 mm	l_5	5000,1
Z_i	12,3 mm	12,3 mm	l_4	8900,1
a_1	$-0,275 \text{ mm}^{-1}$	$-0,272 \text{ mm}^{-1}$	l_3	770,1
M	-0,0204	-0,0155	l_2	2950,1
C_{s3}	-0,68 mm	18 mm	l_1	340,1
C_{c1}	-0,002 mm	-0,83 mm	foil	0,1
C_{s5}		$3,2 \cdot 10^3 \text{ mm}$	r_1	340,1
C_{c2}		$5,3 \cdot 10^2 \text{ mm}$	r_2	2950,1
			r_3	770,1
			r_4	9000,1
			r_5	1000,1

In fig. 15 it is shown probe size versus the probe current divided by transmission ratio of current through the foil. The latter is equal to the current incident on the foil

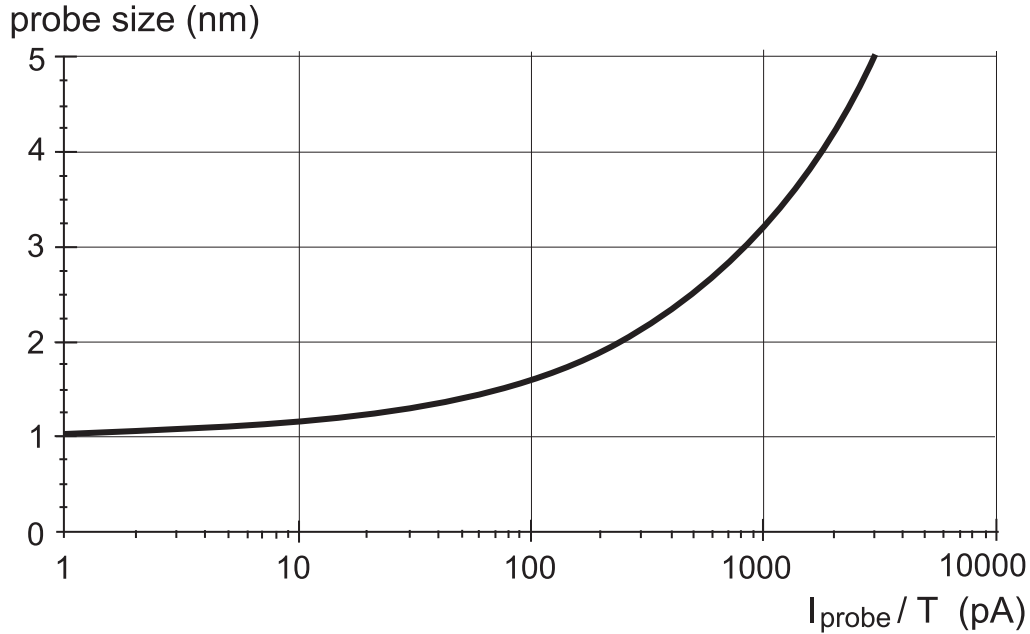


Fig. 15. Probe size versus the probe current divided by transmission ratio of current through the foil

The optimal semi convergent angle is 0,021–0,026 rad, and $WD \approx 1,8 \text{ mm}$.

The above examples clearly show advantages originating from thin film application. However, for practical realization of a SEM, and even more so array

of microcolumns, a lot of improvements has to be done yet. That concerns both construction of electron optical components and technology process for their embodiment.

The detectors

For transforming a microcolumn into SEM is necessary to equip it with appropriate detector of secondary and back scattered electrons (SE and BSE) as it sketched in fig. 2.

Besides small size the SE and BSE detector has to fulfill all common requirements: high collection efficiency, high gain at low voltages, fast response time and linearity in wide range of beam current. The most promising contender seems to be micro channel plate (MCP) and pin diode connected in a tandem manner. Particular construction of detector and technology process for its manufacturing and assembling with microcolumn has to be developed.

The technology for microcolumn manufacturing

So far for microcolumn manufacturing were used or hybrid technology or MEMS technology. Each of those approaches has merits and demerits, which are well known to those skilled in the art, so it is not discussed here in details. We have being developing a technology similar to that in micro electronics, which seems to be more suitable for mass production. Have been developed technology process for lenses shown in fig. 8. (see fig. 16 and 17).

Also have been developed electrostatic octopole deflector–stigmator with thickness of electrodes about $10\ \mu\text{m}$, sketched in fig. 18 and 19. Is assumed to implement two identical pieces placed between lenses in order to achieve deflection simultaneously with stigmatation.

Conclusion

Since 1990-th when first miniaturized lenses have been micromachined, a substantial progress has been achieved in both methods for analytical computations of performance micro electron optics and prototyping of individual electron optical elements. As for arrayed microcolumns, the only example of matrix 4×4 microcolumns for lithography purposes was presented by T.H.P. Chang and alii at 2000-th.

Nevertheless, in the foreseeable future one can expect the appearance of the systems manufactured by more advanced technology.

By our opinion the progress in this area would be determined by technology starting from manufacturing individual components and ending with assembling complete system. So when developing technology for any element as cathode, lens or detector is necessary to think from the beginning about its compatibility with whole technology process.

Two electrode microlens design.

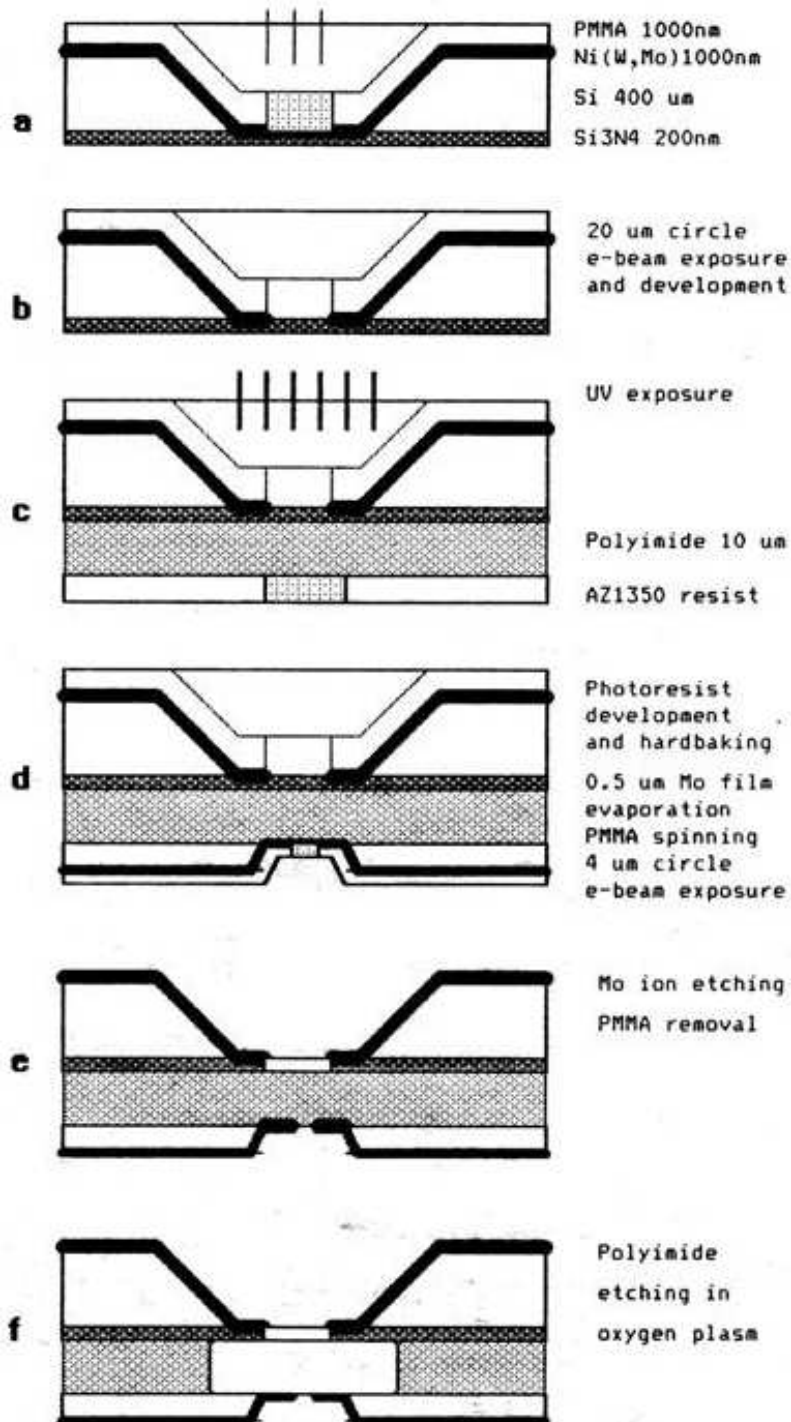


Fig. 16. Non symmetrical two electrodes lens design

Two electrode 100 micrometer microlens design.

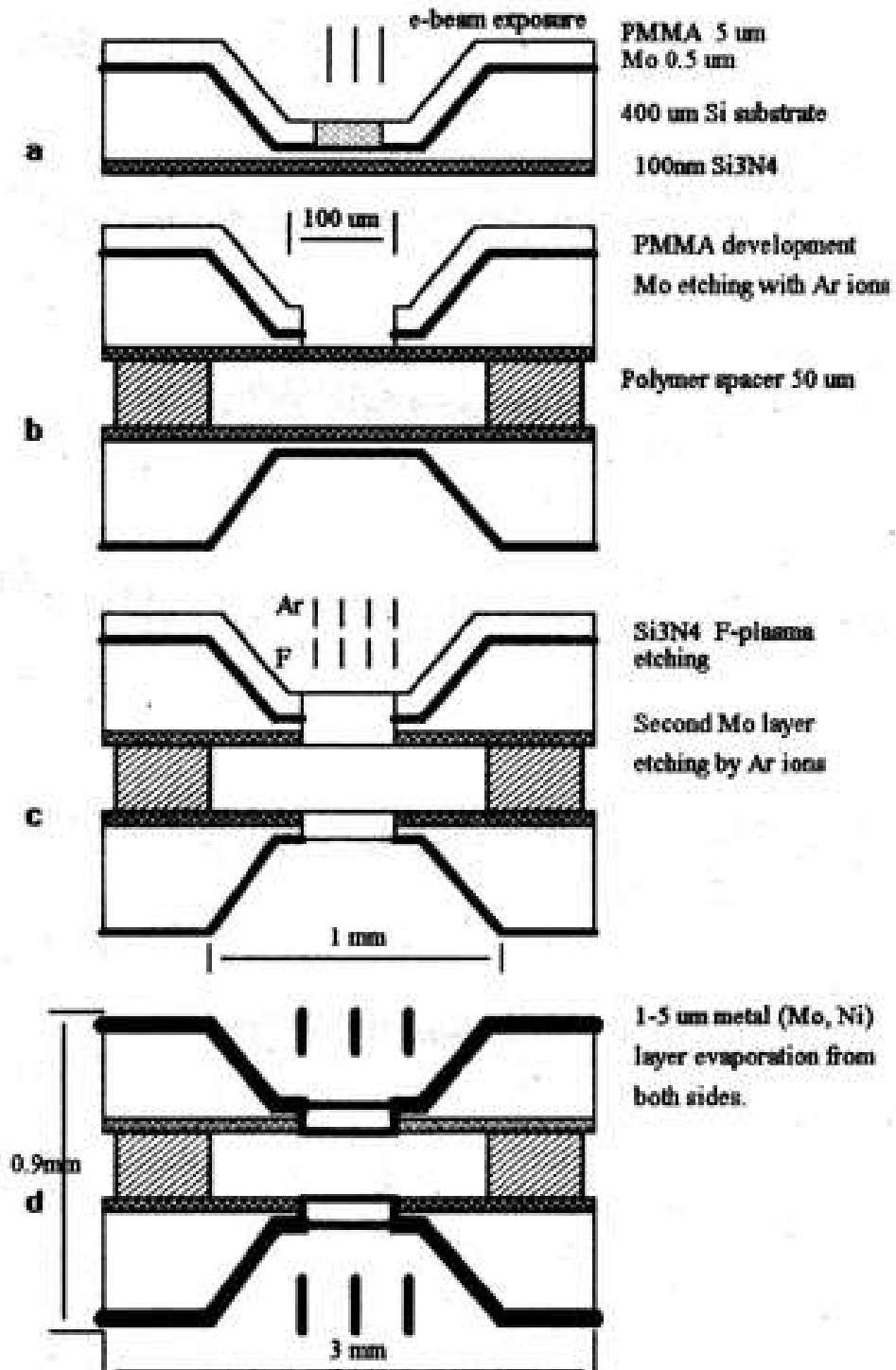


Fig. 17. 100 μ m micro lens design

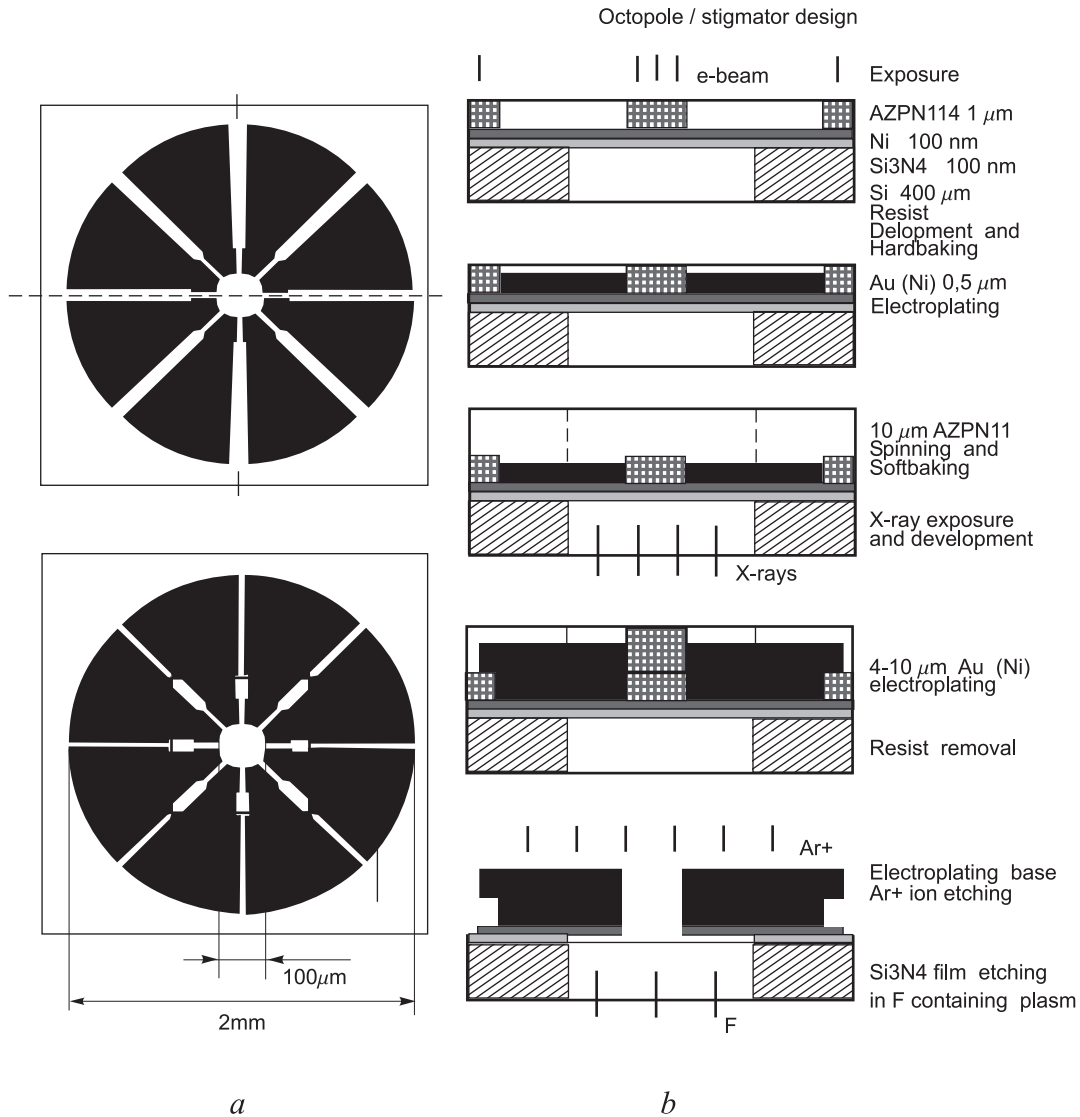


Fig. 18. Design of octopole stigmator. Top view (a) and axial section (b)

References

- [1] *T.H.P. Chang, M.G.R. Thompson, M.L. Yu, E. Kratshmer, et al.* Electron beam microcolumn technology and application // SPIE. Vol. 2522. P. 4–12, (invited paper).
- [2] *G.P.E.M. van Bakel, E.G. Borgonjen, C.W. Hagen, and P. Kruit.* Calculation of the electron-optical characteristics of electron beams transmitted into vacuum from a sharp tip-thin foil junction // J. of Appl. Phys. Vol. 83 (1998) P. 4279.
- [3] *R.H. van Aken, M.A.P.M. Janssen, C.W. Hagen and P. Kruit.* A simple fabrication method for tunnel junction emitters // Solid State Electronics. Vol. 45. (2001) P. 1033.

- [4] *R.H. van Aken, C.W. Hagen, J.E. Barth and P. Kruit.* Low-energy foil aberration corrector // Ultramicroscopy. Vol. 93. (2002) P. 321.
- [5] *R.H. van Aken, C.W. Hagen, J.E. Barth and P. Kruit.* Design of a low-voltage SEM equipped with the low-energy foil corrector // Submitted to Ultramicroscopy.
- [6] *V.V. Aristov, V.V. Kazmiruk, V.A. Kudryashov, V.I. Levashov, S.I. Red'kin, C.W. Hagen, and P. Kruit.* Microfabrication of ultrathin free-standing platinum foils // Surface Science. V. 337. 1998. P. 402–404.
- [7] *H. S. Kim, S. Ahn, D. W. Kim, Y. C. Kim and H. W. Kim, S. J. Ahn.* Sub-60-nm Lithography Patterns by Low-Energy Microcolumn Lithography // Journal of the Korean Physical Society. Vol. 49. P. S712–S715.
- [8] *Ho-Seob Kim, Dae-Wook Kim, Seungjoon Ahn, Sung-Soon Park, Myeong-Heon Seol and Young Chul Kim, Sang-Kook Choi and Dae-Yong Kim.* Multi-Beam Microcolumns Based on Arrayed SCM and WCM // J. of the Korean Physical Soc. Vol. 45, No. 5. P. 1214–1217.
- [9] *V.V. Kazmiruk, T.N. Savitskaja.* arXiv:0805.0248v1 [physics.ins-det].
- [10] *J.E. Barth.* Private communication.
- [11] *V.V. Dremov, V.A. Makarenk, S.Y. Shapoval, O.V. Trofimov, V.G. Beshenkov and I.I. Khodos.* Sharp and clean Tungsten Tips for STM investigation // Nanobiology. Vol. 3. (1994) P. 83–88.
- [12] *R.H. van Aken, M. Lenc and J.E. Barth.* Aberration integrals for the low-voltage foil corrector // Nuclear Instruments and Methods in Physics Research A. Vol. 519. (2004) P. 205 and Vol. 527 (2004) P. 660.